Newton-Marchenko-Rose Imaging

Jyoti Behura[†]*, Kees Wapenaar*[‡] *and Roel Snieder*[†]
[†]*Center for Wave Phenomena, Colorado School of Mines;* [‡]*Delft University of Technology*

SUMMARY

Using only surface reflection data and first-arrival information, we generate up- and down-going wavefields at every image point using the algorithm of Rose (2002b,a) and Wapenaar *et al.* (2011, 2012a). An imaging condition is applied to these up- and down-going wavefields directly to generate the image. Since the above algorithm is based on exact inverse scattering theory, the reconstructed wavefields are accurate and contain all multiply scattered energy in addition to the primary event. As corroborated by our synthetic examples, imaging of these multiply scattered energy helps illuminate the subsurface better than reverse-time migration. We also demonstrate that it is possible to perform illumination compensation using our imaging algorithm that results in improved imaging at large depths.

INTRODUCTION

Wapenaar *et al.* (2011) propose a methodology for reconstructing the 3D impulse response for any "virtual source" in the subsurface using surface reflection data and the direct arrivals from the "virtual source" to the receivers on the surface. Their proposal is the 3D extension of the 1D iterative algorithm of Rose (2002b,a) who shows that in layered media, it is possible to focus all the energy at a particular time (or depth if the velocity is known) by using a complicated source signature.

It is imperative to briefly discuss the pioneering work of V. Marchenko, R.G. Newton, and J.H. Rose on inverse scattering theory (Prosser, 1969; Gopinath & Sondhi, 1971; Burridge, 1980; Bojarski, 1981; Newton, 1989) that is instrumental in the development of the methodology of Rose (2002b,a) and Wapenaar *et al.* (2011, 2012a) and the imaging algorithm presented here. In 1D scattering theory, Marchenko's integral equation (Marchenko, 2011) determines the relation between the wavefield in the interior of a medium and the reflected impulse response. Newton (1980, 1981, 1982) derived a similar relation, called as the Newton-Marchenko integral equation, that uses all scattered waves (reflected and transmitted) in 2D and 3D media. In 1D, this relation is given by

$$u^{+sc}(t,e,x) = \sum_{e'=-1,1} R(t+e'x,-e',e) + \sum_{e'=-1,1} \int_{-\infty}^{\infty} R(\tau+e'x,-e',e)\, u^{+sc}(\tau,e',x)\,\mathrm{d}\tau, \quad (1)$$

where t is time, e is the direction of wave propagation, x is the 1D space, u^{+sc} represents the scattered wavefield, and R is the impulse response function. A physical explanation of the above inverse scattering theory was provided by Rose (2002b,a) who showed that the ideas of focusing and time-reversal in fact result in the Newton-Marchenko equation.

The first step involved in solving for the scattering potential is to solve the Newton-Marchenko integral equation and find the wavefield everywhere inside the medium. Newton (1980, 1981, 1982) solved the inverse scattering problem for the Schrödinger wave equation by combining the Newton-Marchenko integral equation with high-frequency asymptotics. A significant breakthrough was made by Rose (2002b,a) who proposed an iterative approach, which he named 'single-sided' autofocusing, that determines the wavefield in 1D media by focusing the incident wave at a specified time. Rose proved that the incident wave that focuses the wavefield in the interior comprises of a delta function (band-limited in practice) followed by the time-reversed solution of the Marchenko equation. Rose's algorithm was recently implemented on 1D seismic data by Broggini *et al.* (2011) who again show that a 'virtual source' response can be generated from surface reflection data alone. Besides extending Rose's iterative algorithm to higher dimensions, Wapenaar *et al.* (2011, 2012a) also showed that the wavefield at any interior location can also be decomposed into the up- and down-going wavefields.

Here, we show how the up- and down-going wavefields can be used directly for imaging the subsurface. In honor of the contribution of Newton, Marchenko, and Rose, we call the imaging algorithm introduced here as Newton-Marchenko-Rose Imaging, NMRI[1] in short. Besides demonstrating our imaging technique on synthetic examples, we discuss its advantages over existing imaging methods, in particular reverse-time migration (RTM).

ALGORITHM

Any seismic imaging algorithm consists of two steps - wavefield reconstruction and imaging condition. For example, RTM is a two-way imaging technique that utilizes wavefields reconstructed in time by accurately implementing the wave equation (Baysal *et al.*, 1983; Whitmore, 1983; McMechan, 1983) in a smooth velocity model. Wavefield reconstruction in RTM is followed by the application of an imaging condition (commonly cross-correlation) to image the reflectors.

In NMRI, the up- and down-going wavefields are constructed at every location in space using the recipe of Wapenaar *et al.* (2011, 2012a). An imaging condition is applied to these two wavefields to obtain the image. The pseudo-code for NMRI is given in Algorithm 1.

In NMRI, as the complicated incident wavefield focuses at the imaging point, a reflection is generated depending on whether there is actually a reflector at that point in space. In the presence of a reflector, the incident wavefield generates a reflected-wave going in the direction opposite of

[1]NMRI also stands for Nuclear Magnetic Resonance Imaging which is a medical imaging technique.

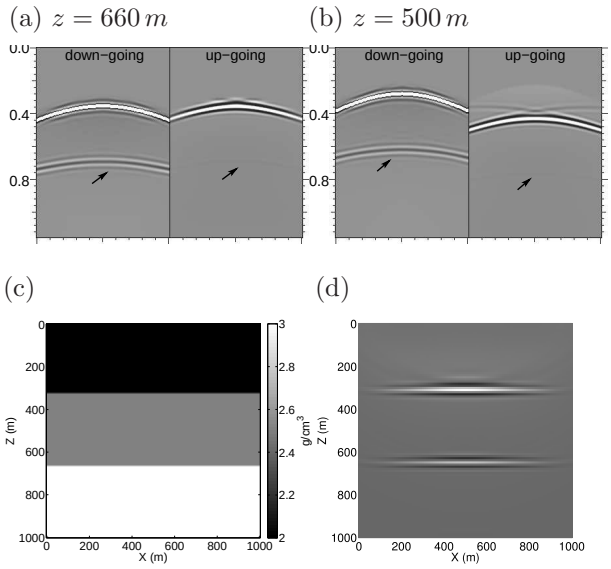

Fig. 1: Up- and down-going wavefields at a reflector position (a) and a depth devoid of reflectors (b). The arrows point to parts of the wavefield generated from internal multiples. (c) The density model of the subsurface and (d) the NMRI image. A constant velocity of 2000 m/s was used for modeling and imaging. Since the normal-incidence reflection coefficient is approximately 0.1 for both reflectors, the internal multiples are weak.

the incident wave; while in the absence of a reflector, no reflected waves are gererated at the image point. Therefore, only at a reflector location the incident-wavefield coincides with the reflected-wavefield which gives rise to a non-zero zero-lag cross-correlation (Figure 1a).

Since the Newton-Marchenko equation is based on exact inverse scattering, the reconstructed wavefields contain all multiply-scattered energy. Note the presence of these multiples in Figures 1a and 1b. Any multiply-scattered wave that is incident on a scatterer will also have a corresponding scattered wave occuring at the same time. In Figure 1a, the multiply-scattered incident- and reflected-waves occur at the same time, while in Figures 1b, they do not coincide in time. Hence, in addition to the primary wavefield, all multiply-scattered energy will also be imaged accurately using NMRI. Other advantages of NMRI are discussed later.

NMRI IN ACTION

Here, we present three synthetic data results to demonstrate the performance and effectiveness of NMRI. The layer-cake (Figure 1) and Lena (Figure 3) models are constant velocity, variable density models while the fold model (Figure 2) has a variable velocity and constant density. The data acquisition is a fixed surface spread in each case where the sources and receivers are at $z = 0m$. The source and receiver spacing is $10\,m$ in all the three acquisitions. Time sampling is also the same ($0.004\,s$) in each case. The direct arrivals were muted from the shot gathers. Besides this, no other processing was

Algorithm 1 Algorithm for NMRI. Superscript "-" represents time reversal and "*" depicts convolution. R is the reflection response.

for any x,y,z in image space **do**
  Compute initial incident wavefield u_0^i from first-arrivals
  $u_{1,2}^i \leftarrow u_0^i$, $u_{1,2}^s \leftarrow 0$
  repeat
    Mute $u_{1,2}^s$ beyond first arrival
    Update incident wavefield:
      $u_1^i \leftarrow u_0^i - u_1^{s-}$,$u_2^i \leftarrow u_0^i + u_2^{s-}$
    Updated scattered wavefield:
      $u_1^s \leftarrow u_1^i * R$,$u_2^s \leftarrow u_2^i * R$
  until $u_{1,2}^s$ converge
  Compute u_{up}, u_{dn} using the recipe of Wapenaar *et al.* (2011,2012)
  Apply imaging condition to u_{up} and u_{dn}
end for

performed on the data; the data contain all orders of internal multiples.

Ray-tracing was used in computing the first breaks for the layercake model and for Lena; for the fold model, the first breaks were computed using a finite-difference wave-propagation code in a smoothed version (Figure 2b) of the true velocity model.

Note that NMRI produced a satisfactory image (Figures 1d,2c, and 3d) in each case. Some steeply-dipping events were not imaged accurately for the fold model and for Lena because of the lack of illumination of these features. Application of a low-cut filter to Lena (Figure 3e) shows that many small details have been imaged in detail. Even though the reflection data is complicated (Figure 3b) and contains all orders of internal multiples, NMRI imaged the primary as well as all the scattered events appropriately.

ADVANTAGES OVER RTM

True amplitude/AVA: NRMI is based on exact inverse scattering theory and therefore the reconstructed wavefield in the interior of the medium is accurate irrespective of the velocity and density distributions in the subsurface. Hence, the NMRI image should be closer to the true reflectivity of the subsurface. Angle gathers for NMRI can be generated in the same way as in RTM. AVA analysis (on angle gathers) for NRMI, however, should be more reliable because the wavefields are accurate.

Multiples are imaged: As mentioned above, since the wavefields in NMRI are reconstructed accurately, the image should be better than existing imaging algorithms. Also, all orders of multiples are reconstructed and imaged accurately. Reflectors not illuminated by the direct arrival, might be illuminated by internal multiples (Fleury, 2012); these reflectors would be visible on the NMRI image but not on the RTM image. This is also corroborated by the virtual-source imaging of internal multiples of Wapenaar *et al.* (2011) and Wapenaar *et al.* (2012b).Imaging of multiples also renders multiple (both surface-related and inter-bed) prediction and suppression unnecessary. Although, none of the examples presented

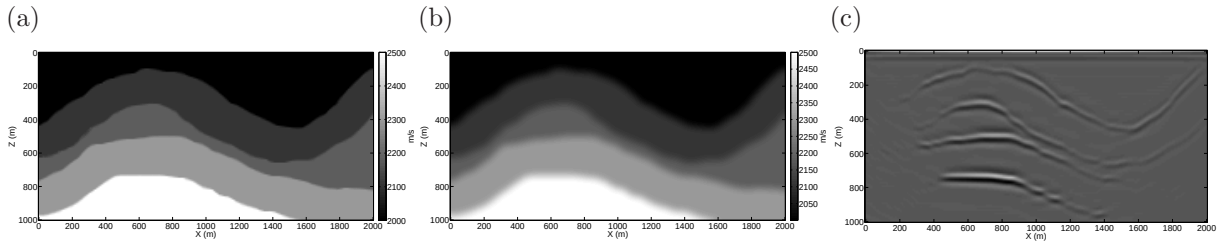

Fig. 2: (a) The original velocity model of the fold system and (b) the smoothed version used for imaging with the corresponding NMRI image (c). A constant density of 1 gm/cm^3 was used in generating the reflection data.

here contain surface-related multiples, the theory underlying NMRI imposes no limitations on the type of multiples.

Illumination compensation: Illumination compensation can be performed by manipulating the amplitude of the leading delta function in the incident wavefield such that each primary arrival at the image point has the same amplitude. By using the same unit delta function for all first arrivals, we ensure that the reflector is equally illuminated from all incidence angles and has the same illumination at all depths. However, if the Green's function is used instead of a uniform delta function, the image at larger depths is poor because of insufficient illumination. For example, Figure 3c generated using the correct Green's function (as the first arrival) can be interpreted as the best possible RTM image (generated from data containing only primary reflections). The above argument explains why the NMRI image (Figure 3d) is significantly better than the best possible RTM image (Figure 3c). Moreover, AVA would become more reliable as all the incident waves have the same amplitude.

Targeted imaging: Since the computation of the first breaks (using ray-tracing or finite-differences) can be done independently for each image point, it is possible to perform targeted imaging using NMRI. The targeted imaging of Lena's left eye is shown in Figure 3f.

Computationally cheap: In NMRI, wavefield computation is done by convolving the incident wavefield with the reflected impulse response for a few iterations (in our tests two iterations were enough in most cases). If ray-tracing is used to compute the incident wavefield, then NMRI would be significantly faster than RTM. A thorough quantitative analysis is necessary to ascertain this.

High frequencies: The cost of RTM increases significantly with increasing frequency content because the extrapolation grid has to be more finely sampled. Wavefield computation using NMRI, on the other hand, has no such limitation because the frequency content of the incident wave and the impulse response are only limited by the temporal nyquist limit.

Highly parallelizable: Since the image at each location in the image space can be computed independently, the algorithm is highly parallelizable in the image space.

Anisotropy: Wavefield extrapolation in anisotropic media using numerical methods is expensive. In addition, depending on the dispersion relation used, the wavefield can contain shear-wave artifacts and incorrect P-wave amplitudes. In NMRI, however, if the first breaks are computed using ray-tracing, then imaging in anisotropic media becomes extremely cheap compared to RTM. Moreover, the wavefields in NRMI are accurate in amplitude even if the medium exhibits velocity anisotropy.

DISCUSSION AND CONCLUSIONS

The first arrivals at the surface from an impulse at any image point can be computed either using ray-tracing or solving the wave equation numerically using finite-differences. In the case of ray-tracing, the incident wavefield can then be designed by convolving the traveltime with a delta function (Rose, 2002b,a). If the background velocity field results in multipathing, one must make sure that the incident wavefield contains all multiple arrivals; if not, the incident wave would not focus at the image point. However, if the first arrivals are computed by numerically solving the wave-equation, one must normalize each incident wave with it's energy content to make sure that all incident waves have similar energy. In the absence of normalization, deeper reflectors will not be imaged properly. First arrivals computed using kinematic ray-tracing might not yield the correct phase; instead, dynamic ray-tracing or gaussian-beam modeling could be used instead. Ray-tracing, however, has one significant advantage: it is substantially cheaper than solving the wave equation numerically (especially in anisotropic media).

Newton-Marchenko-Rose Imaging, which is based on exact inverse scattering theory, shows promise in imaging complicated subsurfaces. Besides primaries, it can be used for illumination compensation and can image both surface-related and internal multiples. This should make NMRI useful for imaging poorly illuminated areas, especially underneath salt bodies. In comparison to RTM, NMRI has other important advantages, such as, it is potentially computationally cheaper, can image arbitrarily anisotropic media, can be used for targeted imaging, and should generate accurate AVA response.

Acknowledgments

The implementation of NMRI was done using freeDDS. Discussions with Farnoush Forghani and Filippo Broggini were very useful. Support for this work was provided by the Consortium Project on Seismic Inverse Methods for Complex Structures at CWP.

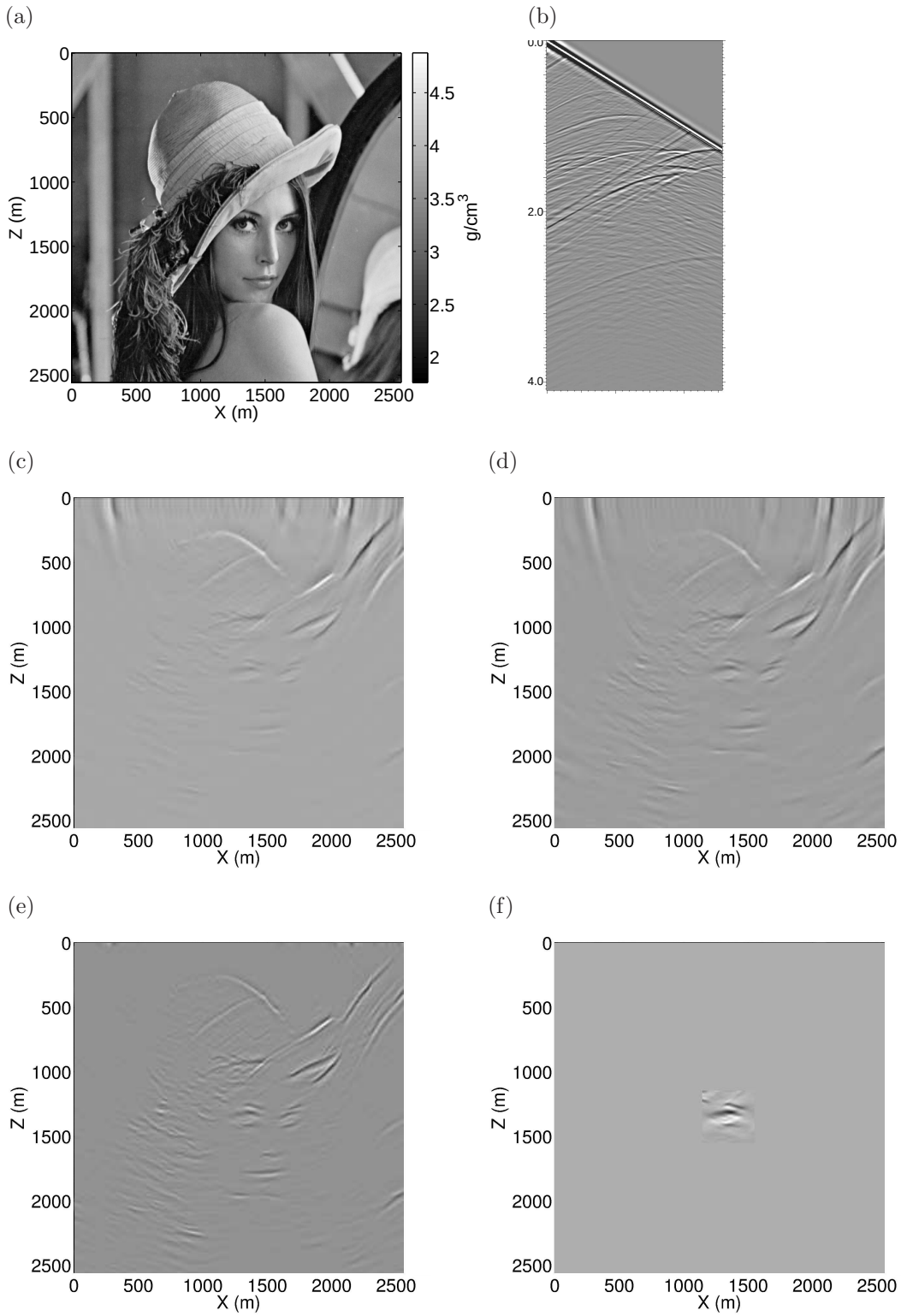

Fig. 3: (a) The density model used in imaging Lena. (b) A sample shot gather. A constant velocity of 2000 m/s was used for modeling and imaging. The NMRI image after one (c) and two (d) iterations. In (c), the Green's function is used for the first arrival while in (d), all the first arrivals are the same delta function. (e) Low-cut filtered version of (d). (f) Targeted imaging of Lena's left eye.

References

Baysal, E., Kosloff, D. D., & Sherwood, J. W. C. 1983. Reverse time migration. *Geophysics*, **48**(11), 1514–1524.

Bojarski, N.N. 1981. Inverse scattering inverse source theory. *J. Math. Phys.*, **22**, 1647–1650.

Broggini, F., Snieder, R., & Wapenaar, K. 2011. Connection of scattering principles: Focusing the wavefield without source or receiver. *SEG Technical Program Expanded Abstracts*, **30**(1), 3845–3850.

Burridge, R. 1980. The Gel'Fand-Levitan, the Marchenko and the Gopinath-Sondi Integral Equations of Inverse Scattering Theory, Regarded in the Context of the Inverse Impulse Response Problems. *Wave Motion*, **2**, 305–323.

Fleury, C. 2012. *Increasing illumination and sensitivity of reverse-time migration with internal multiples*. Tech. rept. CWPXXX. Center for Wave Phenomena, Colorado School of Mines.

Gopinath, B., & Sondhi, M.M. 1971. Inversion of the telegraph equation and the synthesis of nonuniform lines. *Proceedings of the IEEE*, **59**(3), 383 – 392.

Marchenko, V. A. 2011. *Sturm-Liouville operators and applications*. 2 edn. Providence: American Mathematical Society.

McMechan, G. A. 1983. Migration by extrapolation of time-dependent boundary values. *Geophysical Prospecting*, **31**(3), 413–420.

Newton, R. G. 1980. Inverse scattering II. Three dimensions. *Journal of Mathematical Physics*, **21**(7), 1698–1715.

Newton, R. G. 1981. Inverse scattering III. Three dimensions, continued. *Journal of Mathematical Physics*, **22**(10), 2191–2200.

Newton, R. G. 1982. Inverse scattering IV. Three dimensions: generalized Marchenko construction with bound states, and generalized Gel'fand–Levitan equations. *Journal of Mathematical Physics*, **23**(4), 594–604.

Newton, R.G. 1989. *Inverse Schrödinger Scattering in Three Dimensions*. Berlin: Springer Verlag.

Prosser, R.T. 1969. Formal Solutions of Inverse Scattering Problems. *J. Math. Phys.*, **10**, 1819–1822.

Rose, J. H. 2002a. *Time reversal, focusing and exact inverse scattering*. 1 edn. Springer-Verlag, Berlin. Pages 97–105.

Rose, J. H. 2002b. Single-sided autofocusing of sound in layered materials. *Inverse Problems*, **18**, 19231934.

Wapenaar, K., Broggini, F., & Snieder, R. 2011. A proposal for model–independent 3D wave field reconstruction from reflection data. *SEG Technical Program Expanded Abstracts*, **30**(1), 3788–3792.

Wapenaar, K., Broggini, F., & Snieder, R. 2012a. Creating a virtual source inside a medium from reflection data: a stationary-phase analysis. *Geophysical Journal International*, **189**, 001–006.

Wapenaar, K., Thorbecke, J., van der Neut, J., Broggini, F., & Snieder, R. 2012b. Creating virtual sources inside an unknown medium from reflection data: a new approach to internal multiple elimination. *Page submitted of: Extended Abstracts*. European Association of Geoscientists and Engineers.

Whitmore, N. D. 1983. Iterative depth migration by backward time propagation. *SEG Technical Program Expanded Abstracts*, **2**(1), 382–385.